

# Numerical Plasma Dispersion Relation Solver

A. Tomori

Faculty of Mathematics and Physics, Charles University, Prague, Czech Republic.  
Institute of Atmospheric Physics, CAS, Prague, Czech Republic.

**Abstract.** We show first results of our new dispersion relation solver utilizing linear kinetic theory in a hot plasma with a magnetic field. Dispersion relation solutions found using the solver in various modes of calculation, e.g., electrostatic waves without a magnetic field, electromagnetic waves propagating parallel to the magnetic field or general oblique propagation of electrostatic and electromagnetic waves by calculating all components of the dielectric tensor, are compared with results from an older dispersion solver called WHAMP, which uses Padé approximation of the plasma dispersion function. Emphasis is placed on locating instabilities leading to wave growth.

## Introduction

The dispersion relation, a relation between the wave frequency  $\omega$  and the wave vector  $\mathbf{k}$ , yields the possible modes of wave propagation. The frequency is considered complex, with imaginary part  $\Im\{\omega\} \equiv \gamma$  representing the growth (damping) rate. It is usually written in the form  $D(\omega, \mathbf{k}) = 0$ . The reason for this is that the dispersion relation is often obtained as a condition for nontrivial solutions of a homogeneous set of wave equations.

Various properties of a wave can be obtained from the dispersion relation, e.g., the phase and group velocities, the refractive index or whether a wave can propagate under given conditions and if it is damped or amplified.

## Dispersion relation

We will assume a hot homogeneous collisionless plasma with a static magnetic field, which introduces anisotropy. Using the linear kinetic theory (small amplitude waves, no nonlinear effects) and using Maxwell's equations, Vlasov equation and Poisson's equation, the dispersion relation can be derived for example by following steps in *Gurnett and Bhattacharjee* [2005]. By combining Maxwell's equations, the wave equation for electromagnetic waves can be obtained, and the condition for nontrivial solutions mentioned above leads to the requirement that the determinant of the set of wave equations equals zero:

$$\left[ \frac{k^2 c^2}{\omega^2} \left( \frac{\mathbf{k}\mathbf{k}}{k^2} - \mathbf{I} \right) + \boldsymbol{\epsilon}(\omega, \mathbf{k}) \right] \cdot \mathbf{E} \equiv \mathbf{D}(\omega, \mathbf{k}) \cdot \mathbf{E} = 0, \quad (1)$$

$$\det \mathbf{D}(\omega, \mathbf{k}) \equiv D(\omega, \mathbf{k}) = 0, \quad (2)$$

where  $c$  is the speed of light and  $\mathbf{E}$  is the electric field vector. The dielectric tensor  $\boldsymbol{\epsilon}(\omega, \mathbf{k})$  can be expressed using the linear kinetic theory as (*Treumann and Baumjohann* [1997] and in slightly different forms also in *Gurnett and Bhattacharjee* [2005], *Stix* [1992] and *Rönnmark* [1982])

$$\begin{aligned} \boldsymbol{\epsilon}(\omega, \mathbf{k}) = & \left( 1 - \sum_s \frac{\omega_{ps}^2}{\omega^2} \right) \mathbf{I} - \sum_s \sum_{n=-\infty}^{\infty} \frac{\omega_{ps}^2}{\omega^2} \times \\ & \times \int_0^\infty \int_{-\infty}^\infty \left( k_\parallel \frac{\partial F_{s0}}{\partial v_\parallel} + \frac{n\Omega_s}{v_\perp} \frac{\partial F_{s0}}{\partial v_\perp} \right) \frac{\mathbf{S}(v_\perp, v_\parallel)}{k_\parallel v_\parallel + n\Omega_s - \omega} \underbrace{2\pi v_\perp dv_\perp dv_\parallel}_{d\mathbf{v}^3} (+\text{Res}) \end{aligned} \quad (3)$$

where

$$\mathbf{S}(v_{\perp}, v_{\parallel}) = \begin{bmatrix} \frac{n^2 \Omega_s^2}{k_{\perp}^2} J_n^2 & \frac{inv_{\perp} \Omega_s}{k_{\perp}} J_n J'_n & \frac{nv_{\parallel} \Omega_s}{k_{\perp}} J_n^2 \\ -\frac{inv_{\perp} \Omega_s}{k_{\perp}} J_n J'_n & v_{\perp}^2 J_n'^2 & -iv_{\parallel} v_{\perp} J_n J'_n \\ \frac{nv_{\parallel} \Omega_s}{k_{\perp}} J_n^2 & iv_{\parallel} v_{\perp} J_n J'_n & v_{\parallel}^2 J_n^2 \end{bmatrix} \quad (4)$$

and  $\omega_{ps}$ ,  $\Omega_s$  and  $F_{s0}$  represent plasma frequency, gyrofrequency and the unperturbed phase space distribution function of the species  $s$ , respectively. The symbols  $\parallel$  and  $\perp$  denote vector components in the direction parallel and perpendicular to the magnetic field, respectively.

It turns out that evaluating the dielectric tensor is the most difficult part in finding the dispersion relation. It is simplified for some special conditions (which will be discussed in the following sections), but generally it is a tensor with six independent components with integral over velocity space, sum over  $s$  (particle species) and infinite sum over  $n$ . Moreover, the integrand contains Bessel functions  $J_n = J_n(\beta_s)$  and its derivatives  $J'_n = dJ_n(\beta_s)/d\beta_s$ , with argument  $\beta_s = k_{\perp} v_{\perp} / \Omega_s$ .

If there are plasma particles with velocities for which a wave-particle resonance occurs, that is  $k_{\parallel} v_{\parallel} + n\Omega_s - \omega = 0$  (pole in the dielectric tensor (3)), the corresponding complex residue has to be added (the problem with the singularity at resonance was first solved by *Landau* [1946]). The presence of a residue (or the wave-particle resonance) contributes to the imaginary part of the dispersion function  $\Im\{D(\omega, \mathbf{k})\}$ , which in turn directly influences the magnitude of wave growth/damping. This can be shown by a weak growth rate approximation described in *Gurnett and Bhattacharjee* [2005].

### Parallel propagation

In case of parallel wave propagation ( $\beta_s \rightarrow 0$ ), the dielectric tensor  $\epsilon$  can be simplified considerably. It can be shown, that for the term  $nJ_n(\beta_s)/\beta_s$ , which is part of some components of the tensor (4), the following limit is valid

$$\lim_{\beta_s \rightarrow 0} \frac{nJ_n(\beta_s)}{\beta_s} = \begin{cases} 1/2 & n = \pm 1 \\ 0 & \text{otherwise.} \end{cases} \quad (5)$$

Consequently, the infinite sum over  $n$  in (3) reduces to terms with  $n = \pm 1$ , and there are only three nonzero independent components of the dielectric tensor  $\epsilon$  (components  $\epsilon_{11}$ ,  $\epsilon_{12}$  and  $\epsilon_{33}$ ). By building a determinant and requiring it to be equal to zero, three different conditions can be found, which result in the dispersion relations for electromagnetic R and L modes

$$D(\omega, k) = \epsilon_{11} - \frac{c^2 k_{\parallel}^2}{\omega^2} \pm i\epsilon_{12} = 0 \quad (6)$$

as well as a dispersion relation for the electrostatic mode:

$$D(\omega, k) = \epsilon_{33} = 0. \quad (7)$$

Furthermore, if we assume Maxwellian distribution functions (possibly with a drift speed  $v_{ds}$  along the ambient magnetic field), the electrostatic dispersion relation can be even more simplified using the so-called complex *plasma dispersion function*

$$Z(\zeta) = \frac{1}{\sqrt{\pi}} \int_C \frac{e^{-z^2}}{z - \zeta} dz, \quad (8)$$

where the contour  $C$  along the  $z$ -axis is distorted such that it passes below the pole at  $z = \zeta$ . The plasma dispersion function  $Z(\zeta)$  can be found implemented in some numerical program

packages. Then the dispersion relation for electrostatic waves [Gurnett and Bhattacharjee, 2005]

$$D(\omega, k) = 1 - \sum_s \frac{\omega_{ps}^2}{k^2} \int_C \frac{\partial F_{s0}/\partial v_{\parallel}}{v_{\parallel} - \omega/k} dv_{\parallel} \quad (9)$$

can be expressed using the plasma dispersion function  $Z(\zeta)$  as

$$D(\omega, k) = \sum_s \frac{2}{v_{ths}^2} \frac{\omega_{ps}^2}{k^2} [1 + \zeta_s Z(\zeta_s)], \quad (10)$$

where  $\zeta_s = (\omega/k - v_{ds})/v_{ths}$  and  $v_{ths}$  is the thermal velocity  $v_{ths} = \sqrt{\frac{2k_B T_s}{m_s}}$  (with  $k_B$  being the Boltzmann constant and  $T_s$  and  $m_s$  being the temperature and mass of a species  $s$ , respectively).

Thus the dispersion relation for parallel propagation for both electrostatic and electromagnetic waves can be computed significantly faster and easier than for general oblique cases.

## Program

Our numerical dispersion relation solver offers simplified dispersion relation functions for parallel propagation of electrostatic (7) and electromagnetic waves (6), parallel propagation of electrostatic waves with Maxwellian distribution functions of particles (10), and a general form of the dispersion function for oblique propagation (2).

The dispersion function  $D(\omega, \mathbf{k})$  (in all versions) is a complex function of variables  $\mathbf{k}$  and complex  $\omega$ . The roots need to be found numerically (e.g., trying to find values of  $\omega$  for a given  $\mathbf{k}$ , for which  $D(\omega, \mathbf{k}) = 0$ ), thus initial guess values of complex  $\omega$  need to be provided.

The infinite sum over  $n$  in (3) starts with values  $n = 0, -1, 1, -2, 2$ , etc. and can be stopped manually or automatically if magnitudes of subsequent terms in the series fall below a certain limit. Our solver takes advantage of parallel computing while calculating sums over  $s$  and  $n$ .

## Case 1

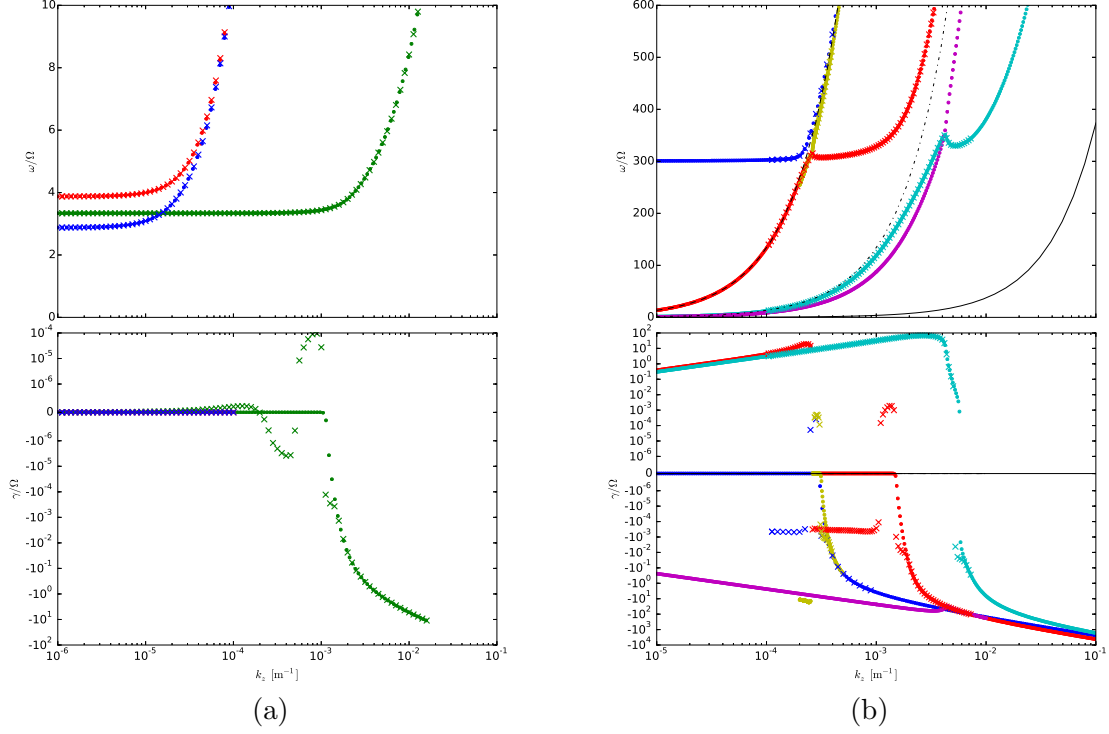
We are comparing results from our numerical dispersion relation solver with results from WHAMP program (R nnmark [1982]). The first example is computed for a plasma having one electron component with the following properties:  $\rho = 0.0279 \text{ cm}^{-3}$ , parallel electron temperature  $T_{\parallel} = 10 \text{ eV}$ , temperature anisotropy  $T_{\perp}/T_{\parallel} = 1$  (i.e., isotropic) and electron cyclotron frequency  $\Omega = 2\pi \cdot 450 \text{ Hz}$ . Solutions for two electromagnetic modes (R and L modes) and the electrostatic Langmuir mode for parallel wave propagation are shown in Fig. 1a.

Filled circles represent results from our solver, whereas the “x” symbols represent the dispersion relation from WHAMP. The branches of real parts (the top graph) match very well. The imaginary branches of our solver and WHAMP disagree at wave numbers where  $\gamma \equiv \Im\{\omega\}$  crosses zero from the positive into the negative regime. This is probably due to round-off errors or approximations used in WHAMP.

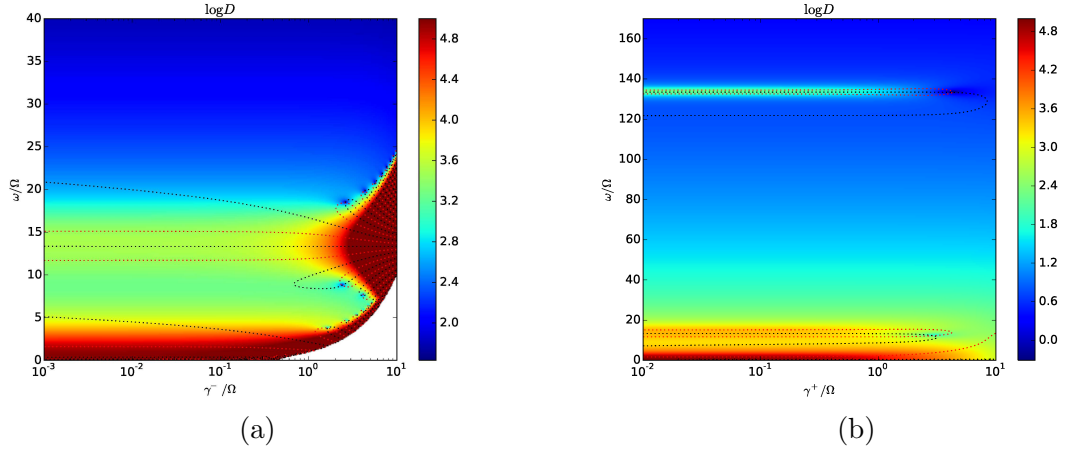
## Case 2

Fig. 1b summarizes result for a plasma having three electron components:  $\rho_{1+2+3} = 0.112 \text{ cm}^{-3}$ ,  $\rho_2/\rho_1 = 10^{-3}$ ,  $\rho_3/\rho_1 = 10^{-1}$ ,  $T_{\parallel 1} = 2 \text{ eV}$ ,  $T_{\parallel 2} = 1 \text{ eV}$ ,  $T_{\parallel 3} = 5 \text{ eV}$  with isotropic temperatures, drift velocities normalized by thermal velocity of the first electron component  $v_{d1}/v_{th1} = 0.28$ ,  $v_{d2}/v_{th1} = 100$ ,  $v_{d1}/v_{th1} = 10$  and electron gyrofrequency  $\Omega = 2\pi \cdot 10 \text{ Hz}$ .

For this case, only the electrostatic modes, i.e., Langmuir (blue) and beam modes (red and cyan), are shown. Results from our solver are again full circles, results from WHAMP are “x” symbols. Real branches from our solver match again very well with those from WHAMP, while



**Figure 1.** Comparison of dispersion relations calculated by our solver (full circles) and by WHAMP (“x” symbols). The dispersion relation is divided into real branch  $\Re\{\omega\}$  (top) and imaginary branch  $\gamma \equiv \Im\{\omega\}$  (bottom). (a) Case 1, electromagnetic (R and L, red and blue) and electrostatic waves (Langmuir, green). (b) Case 2. The electrostatic Langmuir mode (blue) and beam modes (red and cyan) calculated by our solver (full circles) and WHAMP (“x” symbols). A heavily damped mode is shown in magenta. Black lines (solid, dashed and dash-dotted) represent  $\omega = v_{ds}k$ , where  $v_{ds}$  has three different values of drift velocity for the three electron components. The scale of  $y$ -axis in both bottom panels is logarithmic for  $|\gamma/\Omega| > 10^{-6}$  and linear for  $|\gamma/\Omega| < 10^{-6}$  in order to cross zero.



**Figure 2.** Case 2. Shape of the absolute value of the dispersion function  $D(\omega, k = 10^{-4} \text{ m}^{-1})$  of electrostatic waves at fixed  $k$  as a function of real and imaginary components of frequency, for (a)  $\gamma < 0$  and (b)  $\gamma > 0$ . Black and red contours connect points with real and imaginary parts of  $D$  being zero. Roots of  $D$  are at points where both real and imaginary parts are zero (at intersections). Compare with the corresponding graph of the dispersion relation in Fig. 1b — the root at  $\omega \approx (8.8 - 2.4i)\Omega$  in (a) corresponds to magenta points at  $k = 10^{-4} \text{ m}^{-1}$  in Fig. 1b and the two roots in (b) correspond to cyan and red points at  $k = 10^{-4} \text{ m}^{-1}$  in Fig. 1b. The heavily damped magenta branch shown in Fig. 1b is just one of many, as can be seen from the multitude of roots in (a).

# TOMORI: PLASMA DISPERSION RELATION

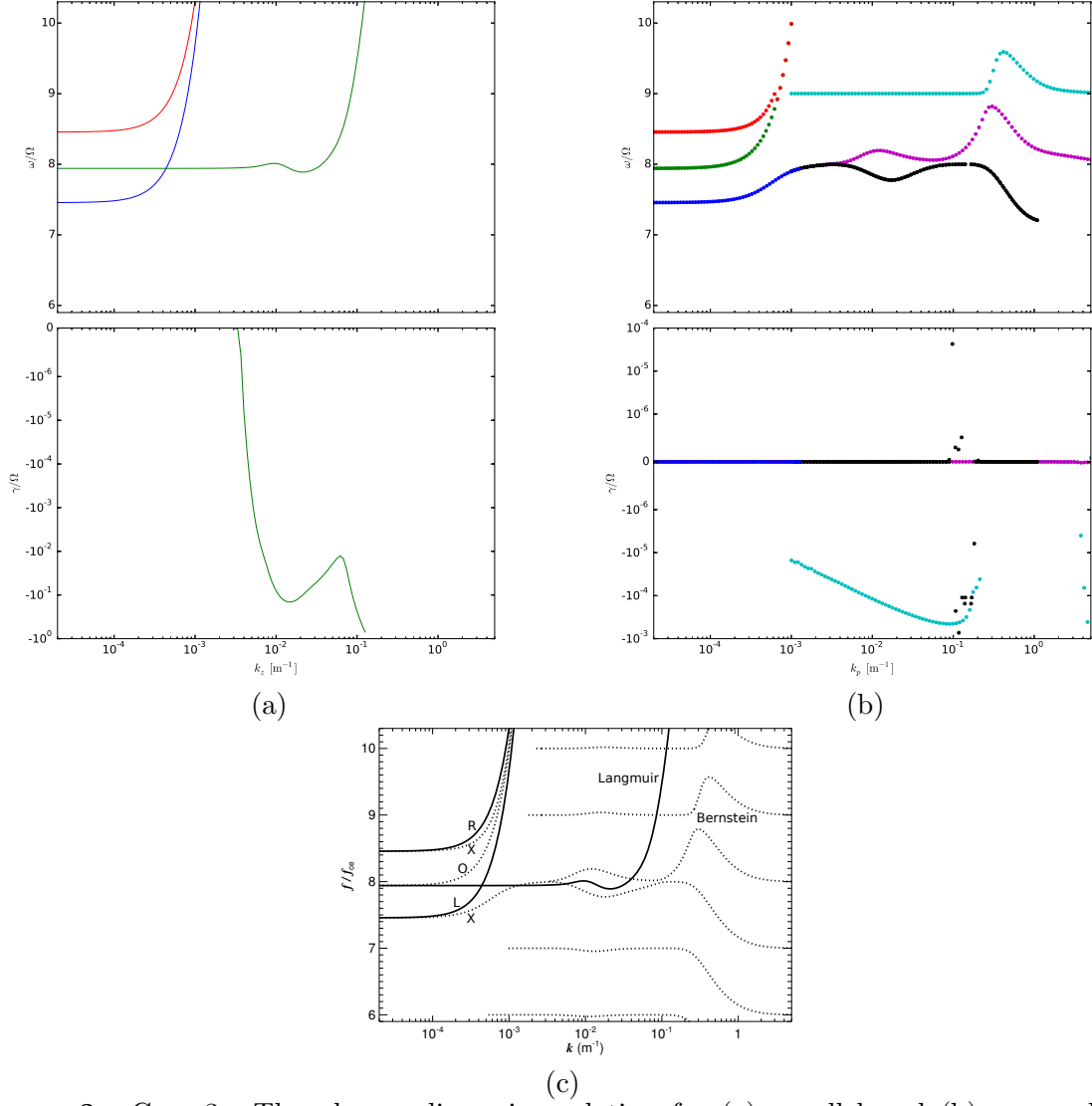


**Figure 3.** Case 3. The plasma dispersion relation for (a) parallel and (b) perpendicular propagation of electrostatic and electromagnetic waves based on plasma parameters taken from *Grimald and Santolik* [2010], calculated by our solver and (c) for comparison calculated by WHAMP. Parallel (solid lines) and perpendicular propagation (dotted lines) are both combined in (c), real part only.

imaginary branches seem to differ again at wave numbers where  $\gamma$  crosses zero from positive into negative regime.

The mode in magenta is heavily damped across the whole range of  $k$ . It turns out that there are many such heavily damped solutions of the dispersion relation, even for a plasma with one electron component. The shape of the dispersion function  $D$  for such a case is plotted in Fig. 2 for a range of complex frequencies (plotted as a function of real and imaginary frequency) for fixed  $k = 10^{-4} \text{ m}^{-1}$  ( $\gamma < 0$  in (a) and  $\gamma > 0$  in (b)). Black and red contours represent points with zero real and imaginary parts of  $D$ , respectively. Roots of  $D$  are located at intersections of those contours. Note the two unstable roots of the dispersion relation for  $\gamma > 0$  in (b) and a series of heavily damped modes for  $\gamma < 0$  in (a), of which just one is shown in the graph of Fig. 1b. Such damped modes have probably no physical meaning.

### Case 3

In a third case we compare the dispersion relation obtained from our solver and WHAMP based on plasma parameters from *Grimald and Santolík* [2010]. The plasma consists of three electron components:  $\rho_{1+2+3} = 48.47 \text{ cm}^{-3}$ ,  $\rho_2/\rho_1 = 1.74\%$ ,  $\rho_3/\rho_1 = 0.868\%$ ,  $T_{\parallel 1} = 10 \text{ eV}$ ,  $T_{\parallel 2} = 1180 \text{ eV}$ ,  $T_{\parallel 3} = 1890 \text{ eV}$ ,  $T_{\perp 1}/T_{\parallel 1} = 0.08$ ,  $T_{\perp 2}/T_{\parallel 2} = 0.98$ ,  $T_{\perp 3}/T_{\parallel 3} = 1.16$  and electron cyclotron frequency  $\Omega = 2\pi \cdot 7875 \text{ Hz}$ . See Fig. 3 for the dispersion relation calculated by our solver (a, b) and by WHAMP (c) (real part only).

Here the most general form of a dispersion function was used — electrostatic and electromagnetic waves for parallel and oblique (near perpendicular) direction. Visible are: (a) the electromagnetic R and L modes and the electrostatic Langmuir mode at parallel propagation, and (b) the electromagnetic X and O modes and electrostatic Bernstein modes at perpendicular propagation. Real parts of branches again seem to match well. For comparison, the results of *Grimald and Santolík* [2010] are displayed in (c), which were obtained with WHAMP.

### Conclusion

We developed a numerical solver of the dispersion relation based on linear kinetic theory. For efficiency and selectivity of desired modes various forms of the dispersion function for special conditions are implemented, e.g., electrostatic wave parallel propagation, electrostatic parallel based on plasma dispersion function  $Z$  (for Maxwellian particle distribution functions), electromagnetic parallel R and L modes selectively and general oblique propagation.

Consistency with the well-established WHAMP solver is observed in real parts of dispersion relations, while in imaginary parts dispersion relations tend to differ at wave numbers where imaginary frequency  $\gamma$  crosses zero from the positive into the negative regime, with the reason being probably round-off errors or approximations used in WHAMP. However, for obliquely propagating modes, which involve summation over a large range of  $n$ , accuracy of results is so far only limited by available computational resources.

### References

- Grimald, S. and Santolík, O., Possible wave modes of wideband nonthermal continuum radiation in its source region, *Journal of Geophysical Research (Space Physics)*, 115, 6209, 2010.
- Gurnett, D. and Bhattacharjee, A., *Introduction to plasma physics: with space and laboratory applications*, Cambridge University Press, 2005.
- Landau, L., On the vibration of the electronic plasma, *J. Phys. USSR*, 10, 25, 1946.
- Rönnmark, K., Waves in homogeneous, anisotropic multicomponent plasmas (WHAMP), Tech. rep., 1982.
- Stix, T., *Waves in plasmas*, American Institute of Physics, 1992.
- Treumann, R. and Baumjohann, W., *Advanced space plasma physics*, Imperial College Press, 1997.